

JKSUS

by MUHAMMAD UZAIR

Submission date: 01-Oct-2023 09:12PM (UTC+0500)

Submission ID: 2181907162

File name: 4_Manuscript-07042023_Clean_Copy.docx (4.86M)

Word count: 8285

Character count: 46366

1 CRISPR/Cas9 mediated *TaRPKI* root architecture gene 2 mutagenesis confers enhanced wheat yield

3 Abstract

4 CRISPR/Cas9 system has been emerged as an efficient tool for sustainable crop improvement.
5 Roots are the “principal hidden organ” that has a crucial function in vascular plants. *Receptor-*
6 *like protein kinase 1 (RPKI)* has been reported to regulate root architecture system (RAS),
7 abiotic stress, and yield in *Arabidopsis* and rice. We employed a CRISPR/Cas9-based system,
8 namely LR-1 and LR-2 constructs having double guided RNAs transformed via agrobacterium
9 for targeted mutagenesis of *TaRPKI* genes in order to alter the root architecture and hence
10 yield in *Triticum aestivum*. Sequencing confirmed seven CRISPR/Cas9-based mutated T0 lines
11 of LR-1 constructs and six T0 lines of LR-2 constructs, with an overall mutation efficiency of
12 41.93%. The T0 plants displayed higher monoallelic mutation compared to the diallelic
13 mutation. 37.5% monoallelic mutation at target site 1 within the D genome by gRNA1 was
14 observed by the LR-1 construct. The LR-2 constructs showed a higher monoallelic mutation
15 frequency of 26.67% at target sites 1 and 2 within A, B, and D genomes. The deletions were
16 mainly short, however longer deletions such as 12d, 17d, 19d, and 20d were detected by
17 gRNA2 of LR-1 construct. Transgenic lines revealed significant alteration in morphology and
18 RSA with a significant increase in number of effective tillers, grain weight, root length, root
19 depth, root volume, and root surface area while reduced root diameter, root angle, and spike
20 length, compared to the wild plants. This significant elevation for tillers and total grain weight
21 proposed that edited lines uplifted grain yield which was caused by to decrease in spike length.
22 The study validates that CRISPR/Cas9 mediated targeted editing of *TaRPKI* is a practical
23 approach for modifying RAS and hence yield enhancement in wheat.

24 **Keywords:** *RPKI* editing; Wheat; Agrobacterium-mediated transformation; Root architecture;
25 grain weight.

26 1. Introduction

27 Roots are the “principal hidden organ” that has a crucial function in vascular plants.
28 Roots are integral compnenet, mediating the water and nutrient uptake required for the growth
29 of the plant (Ober et al., 2021). Roots distribution and growth in soil affect the rate of
30 transpiration that modulates water fluxes among the atmosphere and soil (Javaux et al., 2013).
31 Root growth is crucial for the acquisition of water and nutrients from the soil. The root's uptake

32 of nutrients and water modulates the yields of crops which relies on spatial and temporal
33 distribution of roots in soil (Chen et al., 2020). Root system architecture (RSA) encompasses
34 main traits like length, diameter, length density, depth, volume, and surface area that modulate
35 the organization of root structure and are associated with the uptake of nutrients and water
36 (Alahmad et al., 2019, Djanaguiraman et al., 2019, Danakumara et al., 2021). These traits
37 shaping the distribution of roots in soil have been accompanied by the angle of the root
38 (Alahmad et al., 2019). Among several organs of plants studied, drought mainly affects roots
39 because of its direct association with soil. Drought resistance is correlated directly with the
40 diameter of the root, as bulky roots with huge xylem vessels are effective for the nutrients and
41 water acquisition from deep layers of soil during the conditions of rainfall (Maccaferri et al.,
42 2016). The number of root tips and finer roots are the chief elements of the root system which
43 enhances nutrients and water uptake via root volume and surface area (Bishopp and Lynch
44 2015). In addition, deeper rooting is a vital trait of root that permits water acquisition from
45 deeper profiles of soil which enhances crop productivity (Djanaguiraman et al., 2019,
46 Danakumara et al., 2021). Narrow root seminal angle might enhance the acquisition of residual
47 moisture from deep layers of soil during terminal drought situations and might cause yield
48 improvement (Hamada et al., 2011, Alahmad et al., 2019). Whereas, a wide root seminal angle
49 is accompanied by a root system that is shallow and might explore the top layers of soil for
50 nutrients and water uptake during seasonal rainfall (El Hassouni et al., 2018, Alahmad et al.,
51 2019). The total percentage of plants influenced by drought stress have been doubled in the last
52 40 years, 12 million hectares of land lost each year to drought and desertification. Worldwide,
53 approximately 79% displayed variability in grain yield in the harvesting region of wheat due
54 to drought stress (Djanaguiraman et al., 2019). Understanding the contribution and variations
55 in features of roots might aid in enhanced productivity and drought-resistant genotypes
56 development (Fradgley et al., 2020).

57 Monocotyledons and dicotyledons possess different root system architecture. In
58 monocotyledons such as wheat, the root system is comprised of seminal roots (SR) and crown
59 roots (CR), the crown roots arising from shoots basal node (Nehe et al., 2021). The seminal
60 roots infiltrate firstly into the soil and stay functional throughout the plant lifecycle (Maccaferri
61 et al., 2016, Rufo et al., 2020). These function altogether for the nutrients and water intake
62 from the soil. Bread wheat (*Triticum aestivum*) is one of the major grain crops with a production
63 and area of 771.71 million tons and 218.54 million hectares, respectively (FAOSTAT. 2017).
64 Bread wheat is hexaploid ($2n = 6x = 42$, AABBDD) and domesticated about 8000–25000 years

65 ago in the Middle East region. Wheat being originated from diploid progenitor
66 species: *Triticum urartu* (A-genome), *Aegilops speltoides-related* grass (B-genome),
67 and *Aegilops tauschii* (D-genome). Owing to hexaploidy and an abundance of both repetitive
68 and transposable elements, bread wheat has become one of the largest crop plant genomes
69 (16 Gb), making it challenging to work with from a genetics, genomics, and breeding
70 perspective (Schilling et al., 2020). Globally, wheat is an essential crop and more than a quarter
71 of the population relies on it for feed (Brandt et al., 2020, Gabay et al., 2023). Since wheat is
72 the main staple crop, production needs to be enhanced by 2050 by approximately 38% in order
73 to feed the rising population (Djanaguiraman et al., 2019). Among the climatic fluctuations
74 predicted in the future, drought is one of the main challenges that restrict growth and hence
75 crop yield across the world. Drought stress might lead to a considerable reduction in the wheat
76 yield and its impact fluctuates with the duration, intensity, and timing of the stress compared
77 to the stages of the growth of the crop (Danakumara et al., 2021). Globally, approximately 79%
78 displayed variability in grain yield in the harvesting region of wheat due to the fluctuations in
79 temperature and precipitation. Therefore, improvement in root architecture traits, drought
80 tolerance, and high-yield maintenance is a major challenge in the improvement of wheat
81 (Djanaguiraman et al., 2019).

82 Genome editing is the method of creating specific alterations to a known sequence of
83 DNA. These alterations may comprise deletions, insertions, or variations in the sequence of the
84 gene which might result in the desired change in the protein produced (Brandt et al., 2020).
85 Numerous outcomes of editing are attained by sequence-specific engineered nucleases that
86 create targeted double-stranded DNA breaks (DSBs). Sequence-specific nucleases (SSNs) like
87 mega-nucleases, zinc-finger nucleases (ZFN), and transcription activator-like effector nuclease
88 (TALENs) methods of editing genomes were applied broadly in plants. However, recently,
89 Clustered Regularly Interspaced Short Palindromic Repeats (CRISPR) with Cas nucleases have
90 overtaken these SSNs and mediate the targeting of DNA through guide RNAs (gRNA), which
91 is easy to engineer (Malzahn et al., 2019). CRISPR/Cas9 is considered the most prevalent
92 technology for editing genomes globally, due to its simplicity, versatility, specificity, and
93 flexibility (Li et al., 2019). It has been used in numerous plant species including *Arabidopsis*
94 and *Nicotiana* model-plants, and crop species like maize, rice, and wheat (Feng et al., 2013,
95 Nekrasov et al., 2013, Char et al., 2017, Char et al., 2019, Zafar et al., 2020, Uzair et al., 2021,
96 Ibrahim et al., 2022).

97 *RPK1* is a *Receptor-like protein kinase 1*, belongs to the family of LRR-RLKs,
98 comprises six LRR extracellular motifs, a transmembrane domain (TM), and a single
99 cytoplasmic conserved kinase domain in rice (Rahim et al., 2022). Studies have shown that
100 *OsRPK1* is involved in the architecture of roots by negative modulation of polar auxin transport
101 (*PAT*) and auxin accretion in roots (Zou et al., 2014). Suppression of *RPK1* caused the growth
102 and increased plant height and tiller numbers. Enhanced expression caused a reduction in roots
103 apical meristem and immature adventitious and lateral roots (Zou et al., 2014). *AtRPK1*
104 inhibition, in *Arabidopsis thaliana* exhibited enhanced salt tolerance whereas up-regulated
105 plants displayed lower degrees of salt tolerance in comparison to the normal plants (Shi et al.,
106 2014). The *AtRPK1* level enhanced significantly under less water, ABA, high salt, and less
107 temperature (Hong et al., 1997). Lee et al. studied that *RPK1* inhibition deferred significantly
108 ABA-induced senescence (Lee et al., 2011). *AtRPK1* also plays an essential role during the
109 embryogenesis of the cotyledon primordia (Nodine et al., 2007, Nodine and Tax 2008).
110 *AtRPK1* positively modulates the expression of the *CaMI* gene which further modulates ROS
111 production, senescence of the leaf, and ABA response (Dai et al., 2018).

112 The CRISPR/Cas9 system has successfully demonstrated precise gene editing in many
113 plant systems (Kim et al., 2023). The first reported use of CRISPR-Cas9 to produce a stably
114 genome-edited wheat plant was the targeted knockout of the Mildew Locus O (Mlo), conferring
115 resistance to the powdery mildew pathogen *Blumeria graminis f.sp. tritici* (Bgt) (Wang et al.,
116 2014). Since this first report, wheat genes of agronomical and fundamental scientific interest
117 have been targeted using CRISPR-Cas9 technology, such as *TaGW2* to increase grain weight
118 (Zhang et al., 2018), *TaQsdl* to reduce preharvest sprouting (Abe et al., 2019), *CENH3* for
119 haploid plant induction (Lv et al., 2020), *Sal1* for drought resistance (Mohr et al., 2022). To
120 date, *RPK1* disruption via CRISPR/Cas9 system was not employed for wheat to alter its root
121 architecture and related traits. To address the issue, we synthesized two constructs namely LR-
122 1 and LR-2, with two guide RNAs (gRNAs) each, and developed an *In-planta Agrobacterium*-
123 mediated CRISPR/Cas9 system, hence generating successfully targeted mutations in target
124 sites of *TaRPK1* genes in T0 plants with altered root architecture traits and other agronomic
125 traits. We believe that our study has potential application to produce valuable traits in bread
126 wheat and will aid in the improvement of wheat to guarantee global food security.

127 2. Material and Methods

128 2.1 Wheat germplasm and growing conditions

129 The seeds of both drought-tolerant and high-yielding hexaploid bread wheat cultivar
 130 “Pakistan 2013” were obtained from the National Institute of Genomics and Advanced
 131 Biotechnology (NIGAB), National Agricultural Research Centre (NARC), Islamabad,
 132 Pakistan. The control and transgenic (T0) plants were grown in glasshouse at NIGAB. The
 133 environment of the greenhouse was kept under greenhouse conditions for day light period of
 134 16 h with 25 ± 3°C temperature and night period of 8 h with 15 ± 3°C temperature. The plant
 135 growing pots were filled with soil, peat moss, and sand (1:2:1) soil mixture. Experiments were
 136 carried out on complete randomized design (CRD). Three readings were observed for
 137 agronomic parameters including number of effective tillers, plant height, spike length, grain
 138 related traits, and root architecture traits (root length, depth, diameter, surface area, volume,
 139 and root orientation). The main steps involved in CRISPR-based targeted mutagenesis are
 140 summarized in Supplementary Figure S1.

141 2.2 Target selection and guide RNAs designing

142 The sequences of the *RPKI* genes in the A, B, and D genomes of wheat were retrieved
 143 from “Ensemble Plant” through the BLAST of *RPKI* sequences of *Arabidopsis thaliana* and
 144 *Oryza sativa* (Shi et al., 2014, Zou et al., 2014). The sequence of *RPKI* with a significant
 145 percentage ID and low E-value was selected. For unique gRNA synthesis, the gene target sites
 146 were selected from the exon area of *TaRPKI* gene. The gRNAs were designed manually, and
 147 the possible off-target sites were identified using BLAST search
 148 (<https://blast.ncbi.nlm.nih.gov/Blast.cgi>). The CRISPR/Cas9 system provided by Dr. Bing
 149 Yang (Genetics, Development and Cell Biology department, Ames, Iowa State University,
 150 USA) was followed (Char et al., 2019). The gRNA expression cassettes were synthesized
 151 according to pENTR4-gRNA expression vector 21–25 bp complementary oligonucleotides
 152 were synthesized commercially, with *BtgZI* restriction site, TGTT and AAAC at the 5′ ends of
 153 sense and antisense strand, respectively. Similarly, from the 2nd exon, another four oligos were
 154 designed with *BsaI* restriction site, GTGT and AAAC at the 5′ ends of sense and antisense
 155 strand, respectively (Table 1).

156 **Table 1.** Sequences of guide RNA used for expression cassettes construction.

Gene name and gRNA	Guide RNA sequence (5′ to 3′)
TaRPK-gRNA1-F	TGTTCTTGTTGTTCTTGGTGTTC
TaRPK-gRNA1-R	AAACGCAACACCAAGAACAACAAG
TaRPK-gRNA2-F	GTGTCCTATGCTTTCCTTGCTGAT
TaRPK-gRNA2-R	AAACATCAGCAAGGAAAGCATAGG
TaRPK-gRNA3-F	GTGTATGGATGTGTTTGATGTCAG

157 2.3 CRISPR/Cas9 based Vector construction

158 CRISPR/Cas9 system was used for *TaRPK1* gene disruption, in order to unveil its role
159 in wheat. Two cassettes containing ⁵ two single guide RNAs i.e., gRNA1 and gRNA2, and
160 gRNA1 and gRNA3 along with PAM were synthesized from the first and second exon coding
161 region of *TaRPK1*. The pOs-Cas9 and pENTR4 gateway vector system was used for the
162 purpose of editing. The constructs were synthesized following Bing Yang's method (Char et
163 al., 2019), and the Pakistan-13 wheat cultivar was used for transformation. Both the guide RNA
164 cassettes, with a combination of gRNA1 and gRNA2, and gRNA1 and gRNA3 were ligated
165 into the pENTR4 vector separately, using *BtgZI* and *BsaI* sites. Finally, through an LR-
166 recombination reaction, each cassette was inserted into the final destination pOsCas9 vector,
167 thus giving rise to LR-1 and LR2 constructs. The CRISPR/Cas9 constructed vectors comprising
168 both the gRNAs were then delivered into the *Agrobacterium tumefaciens* LBA4404 strain.

169 2.4 Transformation and screening of edited wheat plants

170 The seeds of the Pakistan-2013 wheat cultivar were used following the method of *in-*
171 *planta* transformation (Supartana et al., 2005, Abdul et al., 2011). For *in-planta* transformation,
172 the seeds were first soaked in 70% v/v solution of analytical grade ethanol for 1 minute with
173 constant shaking followed by washing thrice with autoclaved ddH₂O. Seeds were then washed
174 with 50% Clorox for 15 minutes and were allowed to completely dry. Sowing of seeds was
175 done on Murashige and Skoog (MS) solid medium (Murashige and Skoog 1962).

176 The overnight grew liquid cultures of *A. tumefaciens* strain LBA4404 in LB liquid
177 media were centrifuged at 85000rpm/10 min, and the pellets were separately resuspended in
178 liquid MS media to attain an OD₆₀₀ of 0.6. These harvested cells resuspended with MS
179 medium were supplemented with 200µM acetosyringone and mixed gently. For the three-day-
180 old seedlings, the apical meristem part was pierced up to 1mm depth, and agrobacterium
181 inoculum was injected into it. After three days of co-cultivation, seedlings were washed with
182 ddH₂O thrice followed by washing with 500 mg/L cefotaxime antibiotic for 15 min to remove
183 excess bacteria that have grown on co-cultivated seedlings. The seedlings were then shifted to
184 the selection and regeneration medium containing MS salts with vitamins; Sucrose 30g/L;
185 cefotaxime 250µg/mL; BAP 1.5mg/L, kanamycin, and hygromycin. The seedlings were then
186 kept at 28°C with the standard light and dark cycle for four weeks. After one month, the

187 seedlings were transplanted for acclimatization into the growth room, covered with a
188 transparent lid for humidity maintenance. The transformed seedlings were then moved into
189 pots and placed in a greenhouse under a controlled environment (22/16°C with day/night 16/8h
190 photoperiod and 70% humidity) till maturity.

191 For the detection of gRNAs efficiency in wheat plants, a T7 endonuclease I assay was
192 performed (Kim et al., 2018). To confirm the DNA double-strand break, PCR amplicons were
193 gel purified, denatured, reannealed, and treated with T7EI. The PCR amplicons were sequenced
194 to determine the mutation frequency.

195 **2.5 Root architecture traits and morphological parameters determination**

196 The root architecture traits including root length, depth, diameter, volume, surface area,
197 and root orientation were observed in T0 transgenic lines and wild-type plants. For this
198 purpose, pictures from four-week-old wheat seedlings were captured and analyzed with the
199 help of RhizoVision software (Seethepalli et al., 2021). Morphological data measured included
200 the number of effective tillers, plant height, spike length, and 1000-grain weight at the maturity
201 stage. A minimum of three replicates from T0 transgenic lines and control plants were recorded
202 for each trait.

203 **2.6 Statistical analysis**

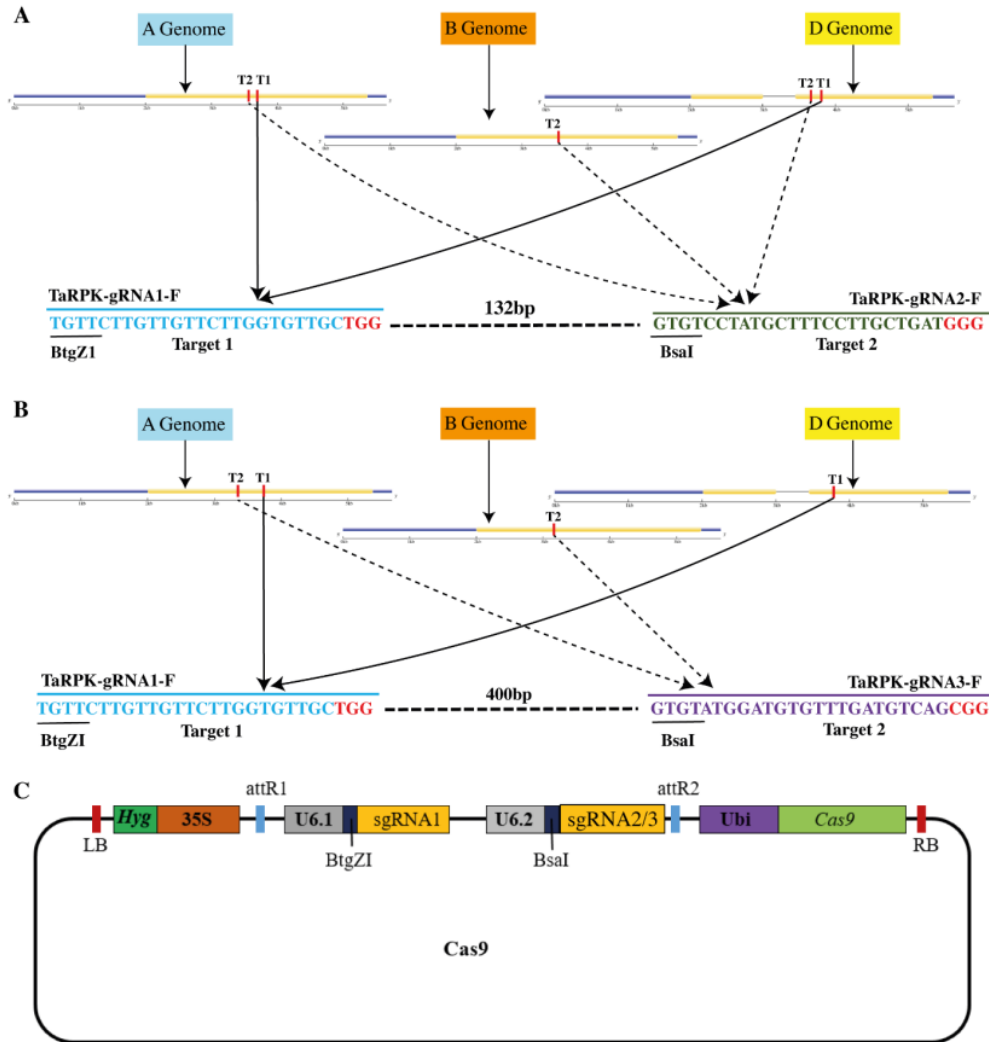
204 All the recorded data was statistically analyzed by using Microsoft Excel 2019. Student
205 *t*-test was performed to determine the significant differences among the samples ($n = 3$, $* = P$
206 < 0.05 , $** = P < 0.01$).

207 **3. Results**

208 **3.1 Selection of target homeolog of *TaRPKI* gene**

209 The *RPKI* sequences in the A, B, and D sub-genomes of wheat retrieved by BLAST
210 from “Ensemble Plant”, with the highest percentage ID and low E-value were located on
211 chromosome 2. TraesCS2A02G176500, TraesCS2B02G202900, and TraesCS2D02G183900
212 wheat sequence Ensemble IDs showed the highest percentage of similarities 86%, 85.5%, and
213 94.1%, respectively (Supplementary Table S1). The coding sequences were aligned and
214 sgRNAs were synthesized from the conserved region. The sgRNA1 was designed from the
215 conserved region of A and D genomes, sgRNA2 from A, B, and D genomes, and sgRNA3 from

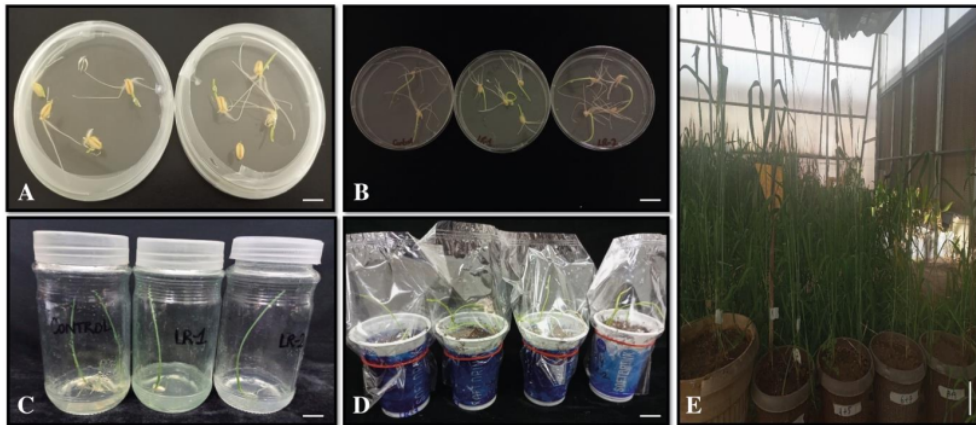
216 the conserved region of A and B genomes (Supplementary Table S2). These sgRNAs were
 217 synthesized from the first exon of the A and B genomes, and the second exon of the D genome
 218 (Figure 1).



219 **Figure 1: Illustration of sgRNA expression cassette.** (A) The representation of *TaRPKI*-gRNA1 (Target
 221 1) and *TaRPKI*-gRNA2 (Target 2) for constructing LR1. (B) Indication of *TaRPKI*-gRNA1 (Target 1) and
 222 *TaRPKI*-gRNA3 (Target 2) for LR2 construct. PAM sites were shown in red color and restriction
 223 endonucleases (*BtgZI* and *BsaI*) recognition sequences were underlined. (C) Schematic illustration of binary
 224 vector transformed into wheat. The constructs *TaRPKI*-gRNA consists of a cassette with Kanamycin
 225 resistant gene, flanked by attR1 and attR2 gateway recombination sequence, inserted into the pOs-Cas9
 226 binary vector via LR recombination reaction. The expression cassette comprises gRNA pairs (*TaRPKI*-
 227 gRNA1 and *TaRPKI*-gRNA2/3) followed by Cas9 endonuclease regulated by Rice Ubiquitin promoter.

228 3.2 CRISPR/Cas9 *TaRPKI* Vector and *In-planta* transformation

229 The binary vector CRISPR/Cas9 containing *TaRPKI*-sgRNAs were constructed
230 accomplished by gateway recombination reaction (Supplementary Figure S2). The first
231 construct with a combination of sgRNA1 and sgRNA2 is termed LR-1, while the LR-2
232 construct contains the sgRNA1 and sgRNA3 expression cassettes, respectively. In planta apical
233 meristem transformation being an easy, cheap, and efficient method for transformation was
234 adopted for transformation using CRISPR/cas9 targeted mutagenesis (Figure 2). More than 25
235 independent lines were obtained by using this technique.



236
237 **Figure 2: In planta apical meristem transformation CRISPR/Cas9 targeted mutagenesis.** (A) Wheat
238 seeds germination on MS medium. (B) Transfer of ex-plant into co-cultivation media. (C) Screening of
239 plants on selection media. Plants with kanamycin and hygromycin resistance survived on selection media.
240 (D) Acclimatization of transplanted seedlings in the growth room, by covering the seedlings with a
241 transparent sheet. (E) Transformed plants shifted to pots in glass house and grown under controlled
242 conditions.

243 3.3 Mutation detection in T0 plants

244 The detection of the edit mutation type was performed after the transformation and
245 regeneration of T0 plants. A total of 31 transgenic plants were obtained from screening of
246 selection antibiotic, 16 of which were of LR-1 constructs and 15 of LR-2 constructs (Table 2).
247 Mutation detection in these transgenic plants was performed by genomic DNA extraction from
248 the leaf tissues of T0 plants (Supplementary Figure S3), followed by designing specific primers
249 flanking target sites of A, B, and D genomes (Supplementary Table S3). The PCR products
250 were digested with T7 endonuclease I (T7EI) assay followed by Sanger sequencing for
251 mutation detection. T7 endonuclease I assay with PCR products did not reveal the expected
252 pattern of digestion for the insertion/ deletion (InDel) mutation. However, Sanger sequencing
253 of the PCR products confirmed seven CRISPR/Cas9-based mutated T0 lines of LR-1 constructs
254 and six CRISPR/Cas9-based mutated T0 lines of LR-2 constructs, with a percentage mutation

255 frequency of 43.75% (7 out of 16), and 40% (6 of 15) for LR-1 and LR-2 constructs,
 256 respectively. The two LR-1 and LR-2 constructs targeting the *RPK1* gene achieved similar
 257 mutation frequency. Overall, these results showed a high mutation efficiency of 41.93%.

258 **Table 2.** Percentage of mutated plants in the T0 generation.

Vector	Target gene	Construct	sgRNA	No. of plants examined	No. of plants with mutations	% Mutation frequency	sgRNA GC content
CRISPR / Cas9	TaRPK1	LR-1	sgRNA1	16	07	43.75%	41.67%/
			sgRNA2				45.83%
		LR-2	sgRNA1	15	06	40%	41.67%/
			sgRNA3				41.67%
Total				31	13	41.93%	

259 **3.4 Types of mutations caused by CRISPR/Cas9**

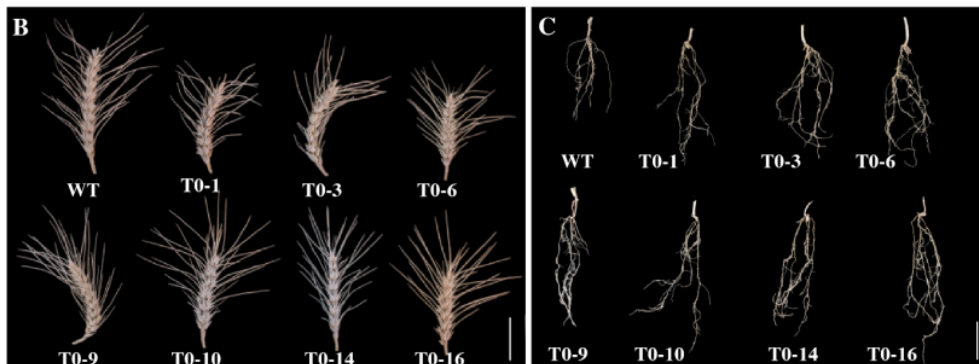
260 The sequencing results showed two types of mutations, deletions, and insertions. The
 261 insertions of one bp, A, and T were detected at target sites (Figures 3-6). The frequency of
 262 insertion was less as compared to that of deletion. Short deletions of one to nine bp were also
 263 observed. The deletions were mostly short, however longer deletions such as 12d, 17d, 19d,
 264 and 20d (figure 3A) were detected in T0-6, T0-10, T0-14, and T0-16 lines. The longer deletions
 265 were observed at target site 2 by sgRNA2 of LR-1 construct, showing high efficiency of
 266 sgRNA2 compared to sgRNA1 and sgRNA3 (Figure 5A). The total deletion ratio was higher
 267 compared to total insertions and Cas9 cleavage sites usually 3 bp upstream of PAM when all
 268 the mutation events were summed. These findings indicate that our CRISPR/Cas9 system did
 269 work in the T0-edited plants.

A

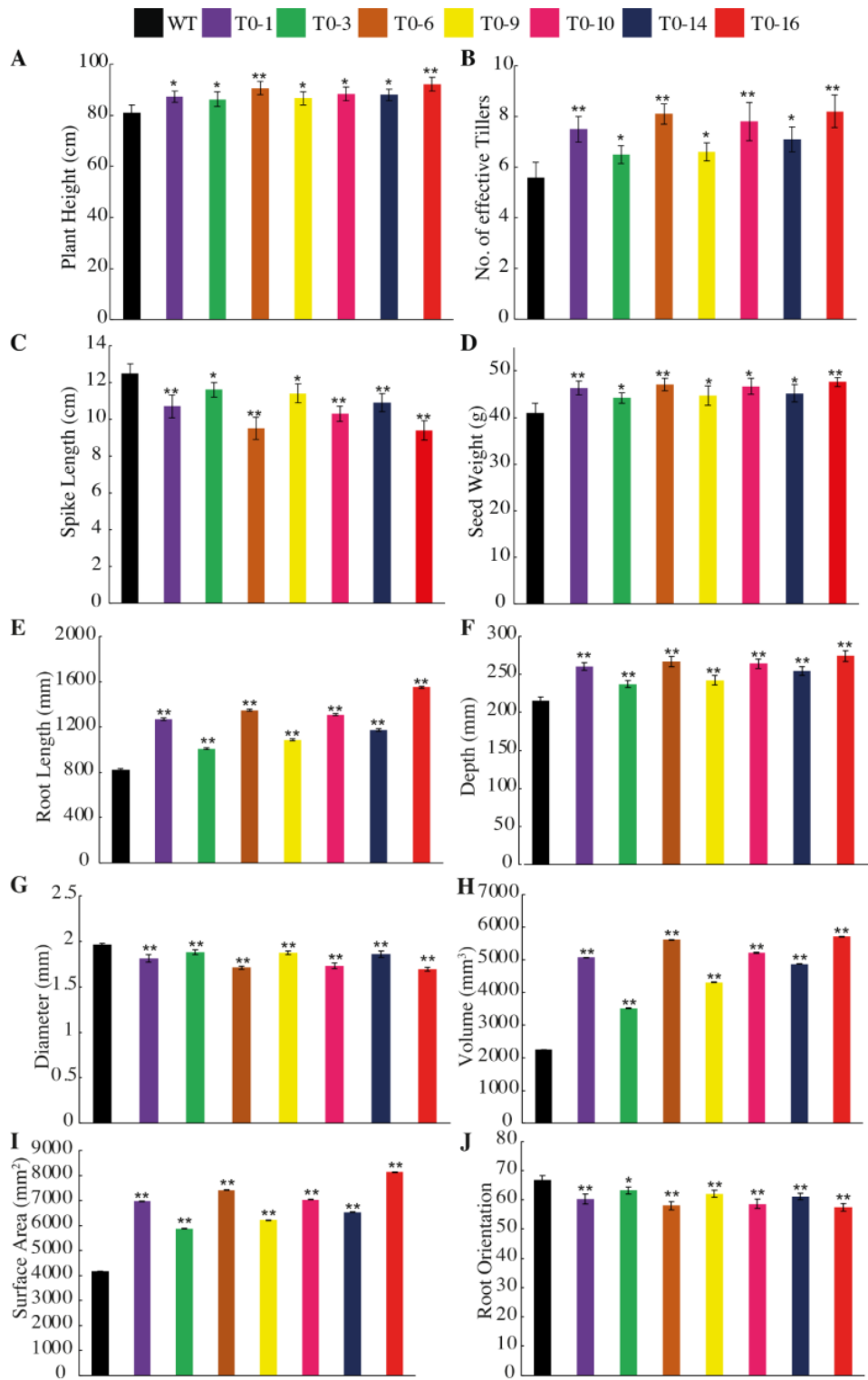
	Target 2	PAM	132bp	Target 1	PAM	
WT	GGGATCCTATGCTTTCCTTGCTGATGGGAATAA	CTTCTCTTGTGTTCCTGGTGTTCGGTAACC			+1/WT
T0-A1	GGGATCCTATGCTTTCCTTGCTGATGGGAATAA	CTTCTCTTGTGTTCCTGGTGTTCGGTAACC			-3/-2
T0-A3	GGGATCCTATGCTTTCCTTGCTGATGGGAATAA	CTTCTCTTGTGTTCCTGGTGTTCGGTAACC			WT/WT
T0-A6	GGGATCCTATGCTTTCCTTGCTGATGGGAATAA	CTTCTCTTGTGTTCCTGGTGTTCGGTAACC			WT/WT
T0-A9	GGGATCCTATGCTTTCCTTGCTGATGGGAATAA	CTTCTCTTGTGTTCCTGGTGTTCGGTAACC			-3/-1
T0-A10	GGGATCCTATGCTTTCCTTGCTGATGGGAATAA	CTTCTCTTGTGTTCCTGGTGTTCGGTAACC			WT/WT
T0-A14	GGGATCCTATGCTTTCCTTGCTGATGGGAATAA	CTTCTCTTGTTCCTGGTGTTCGGTAACC			+1/-2
T0-A16	GGGATCCTATGCTTTCCTTGCTGATGGGAATAA	CTTCTCTTGTTCCTGGTGTTCGGTAACC			-3/-2
	GGGATCCTATGCTTTCCTTGCTGATGGGAATAA	CTTCTCTTGTTCCTGGTGTTCGGTAACC			-12/-4
	GGGATCCTATGCTTTCCTTGCTGATGGGAATAA	CTTCTCTTGTTCCTGGTGTTCGGTAACC			-20/-3
	GGGATCCTATGCTTTCCTTGCTGATGGGAATAA	CTTCTCTTGTTCCTGGTGTTCGGTAACC			-2/WT

	Target 2	PAM	132bp	Target 1	PAM	
WT	GGGATCCTATGCTTTCCTTGCTGATGGGAATAA	CTTCTCTTGTGTTCCTGGTGTTCGGTAACC			+1/
T0-B1	GGGATCCTATGCTTTCCTTGCTGATGGGAATAA	CTTCTCTTGTGTTCCTGGTGTTCGGTAACC			-4/
T0-B3	GGGATCCTATGCTTTCCTTGCTGATGGGAATAA	CTTCTCTTGTGTTCCTGGTGTTCGGTAACC			WT/
T0-B6	GGGATCCTATGCTTTCCTTGCTGATGGGAATAA	CTTCTCTTGTGTTCCTGGTGTTCGGTAACC			-1/
T0-B9	GGGATCCTATGCTTTCCTTGCTGATGGGAATAA	CTTCTCTTGTGTTCCTGGTGTTCGGTAACC			WT/
T0-B10	GGGATCCTATGCTTTCCTTGCTGATGGGAATAA	CTTCTCTTGTGTTCCTGGTGTTCGGTAACC			-19/
T0-B14	GGGATCCTATGCTTTCCTTGCTGATGGGAATAA	CTTCTCTTGTGTTCCTGGTGTTCGGTAACC			-3/
T0-B16	GGGATCCTATGCTTTCCTTGCTGATGGGAATAA	CTTCTCTTGTGTTCCTGGTGTTCGGTAACC			-2/
	GGGATCCTATGCTTTCCTTGCTGATGGGAATAA	CTTCTCTTGTGTTCCTGGTGTTCGGTAACC			WT/
	GGGATCCTATGCTTTCCTTGCTGATGGGAATAA	CTTCTCTTGTGTTCCTGGTGTTCGGTAACC			-6/
	GGGATCCTATGCTTTCCTTGCTGATGGGAATAA	CTTCTCTTGTGTTCCTGGTGTTCGGTAACC			-5/
	GGGATCCTATGCTTTCCTTGCTGATGGGAATAA	CTTCTCTTGTGTTCCTGGTGTTCGGTAACC			+1/
	GGGATCCTATGCTTTCCTTGCTGATGGGAATAA	CTTCTCTTGTGTTCCTGGTGTTCGGTAACC			WT/
	GGGATCCTATGCTTTCCTTGCTGATGGGAATAA	CTTCTCTTGTGTTCCTGGTGTTCGGTAACC			-8/

	Target 2	PAM	132bp	Target 1	PAM	
WT	GGGATCCTATGCTTTCCTTGCTGATGGGAATAA	CTTCTCTTGTGTTCCTGGTGTTCGGTAACC			+1/WT
T0-D1	GGGATCCTATGCTTTCCTTGCTGATGGGAATAA	CTTCTCTTGTGTTCCTGGTGTTCGGTAACC			-4/-1
T0-D3	GGGATCCTATGCTTTCCTTGCTGATGGGAATAA	CTTCTCTTGTGTTCCTGGTGTTCGGTAACC			WT/-2
T0-D6	GGGATCCTATGCTTTCCTTGCTGATGGGAATAA	CTTCTCTTGTGTTCCTGGTGTTCGGTAACC			-6/-1
T0-D9	GGGATCCTATGCTTTCCTTGCTGATGGGAATAA	CTTCTCTTGTGTTCCTGGTGTTCGGTAACC			+1/-4
T0-D10	GGGATCCTATGCTTTCCTTGCTGATGGGAATAA	CTTCTCTTGTGTTCCTGGTGTTCGGTAACC			-5/WT
T0-D14	GGGATCCTATGCTTTCCTTGCTGATGGGAATAA	CTTCTCTTGTGTTCCTGGTGTTCGGTAACC			+1/WT
T0-D16	GGGATCCTATGCTTTCCTTGCTGATGGGAATAA	CTTCTCTTGTGTTCCTGGTGTTCGGTAACC			-17/WT
	GGGATCCTATGCTTTCCTTGCTGATGGGAATAA	CTTCTCTTGTGTTCCTGGTGTTCGGTAACC			-3/WT
	GGGATCCTATGCTTTCCTTGCTGATGGGAATAA	CTTCTCTTGTGTTCCTGGTGTTCGGTAACC			WT/WT
	GGGATCCTATGCTTTCCTTGCTGATGGGAATAA	CTTCTCTTGTGTTCCTGGTGTTCGGTAACC			-9/-5

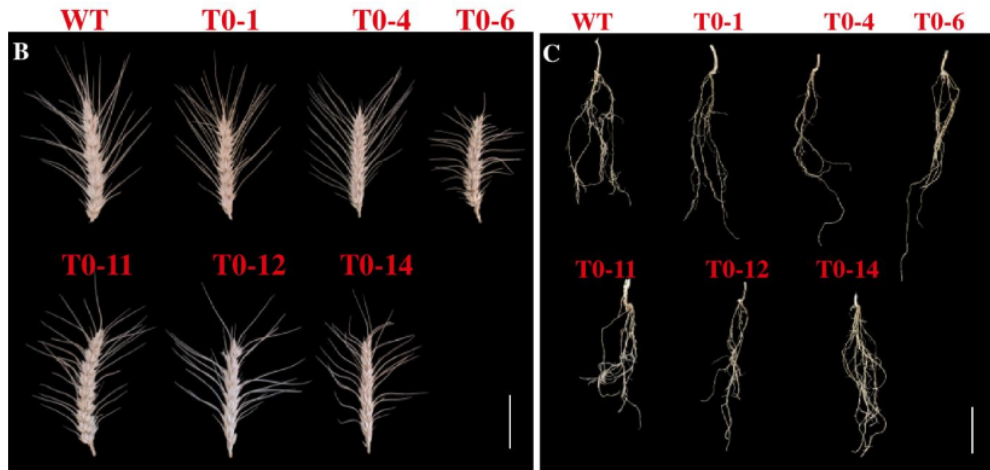


270
 271 **Figure 3:** CRISPR/Cas9 induced targeted mutagenesis of the *TaRPK1* target gene by LR-1
 272 construct within A, B, and D genomes of wheat T0 plants (A). PAM sites were shown in red,
 273 nucleotides in blue denote target site 1 (T1), and nucleotides in orange represent target site 2
 274 (T2). The lowercase letter denotes insertion, dashes represent deletions and dots indicate
 275 nucleotides not shown. Spike architecture of wild type and edited transformed LR-1 T0 lines
 276 (B). Root architecture of wild type and edited transformed LR-1 T0 lines (C).
 277



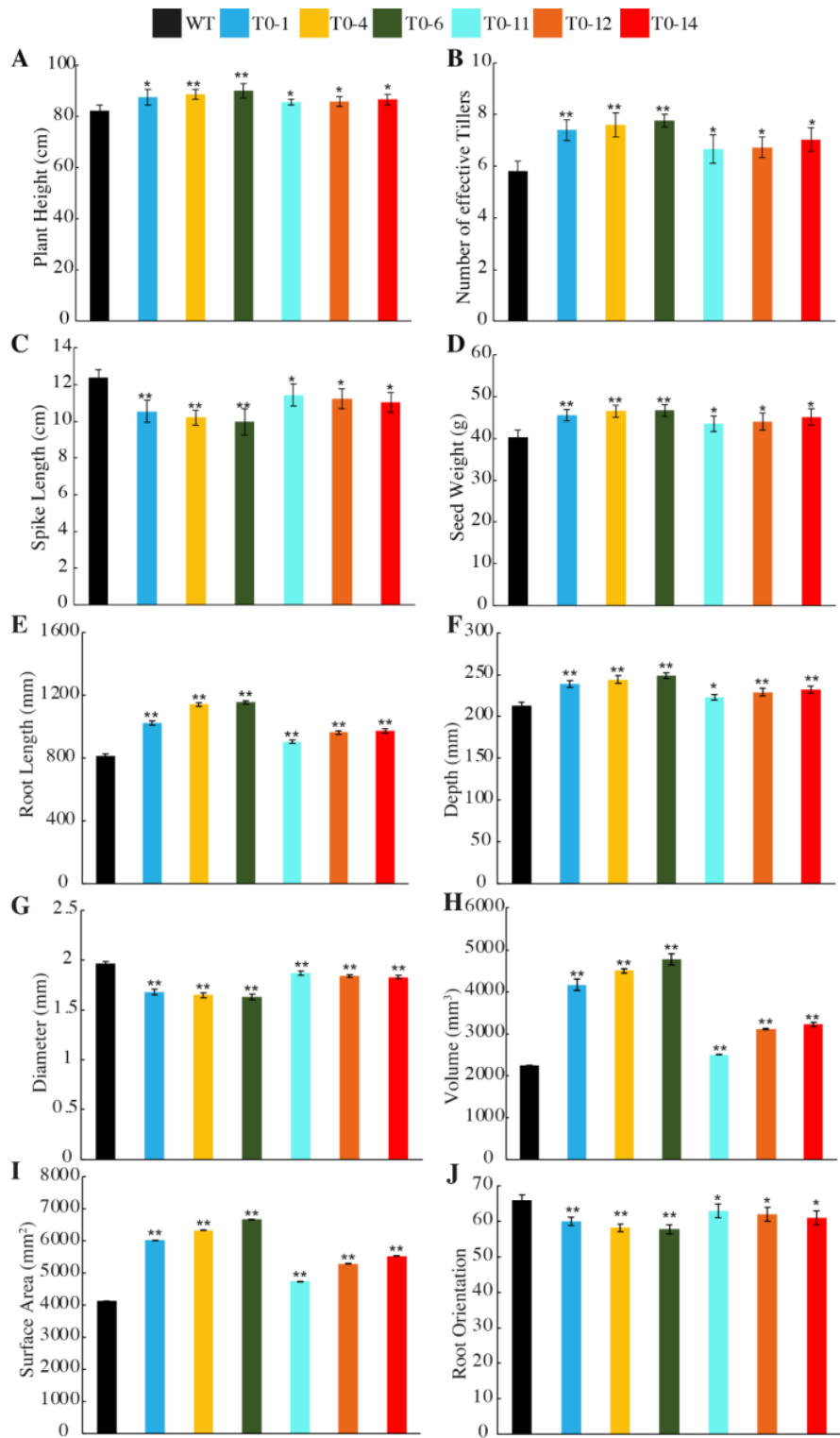
279 **Figure 4:** Phenotypic comparison of LR-1 construct for Plant height (cm, **A**), Number of
 280 effective tillers (**B**), Spike length (cm, **C**), Seed weight (g, **D**), Root length (mm, **E**), Root depth
 281 (mm, **F**), Root diameter (mm, **G**), Root volume (mm³, **H**), Root surface area (mm², **I**), and
 282 Root orientation (**J**) of wild type (WT) and edited T0 lines. The data indicates the mean ± SE
 283 of three biological replicates. Student's *t*-test was used (* = *P* < 0.05, and ** = *P* < 0.01).

	Target 2	PAM	400bp	Target 1	PAM	
A WT	CCTGCATGGATGTGTTTGATGTCAGCGGAAACC.....	CTTCTCTTGTGTGTTCTGGGTGTGCTGGTAACC				
T0-A1	CCTGCATGGATGTGTTTGATGTCAGCGGAAACC.....	CTTCTCTTGTGTGTTCTTGGT -- TGCTGGTAACC				WT/-2
	CCTGCATGGATGTGTTT --- CAGCGGAAACC.....	CTTCTCTTGTGTGTTCTGGGTGTGCTGGTAACC				-4/WT
T0-A4	CCTGCATGGATGTGTTTGATGTCAGCGGAAACC.....	CTTCTCTTGTGTGTTCTGGGTGTGCTGGTAACC				+1/WT
	CCTGCATGGATGTGTT --- CAGCGGAAACC.....	CTTCTCTTGTGTGTTCTGGT --- TGCTGGTAACC				-6/-4
T0-A6	CCTGCATGGATGT - TTTGATGTCAGCGGAAACC.....	CTTCTCTTGTGTGTTCTGGGTGTGCTGGTAACC				-1/WT
	CCTGCATGGATGTGTTT --- CAGCGGAAACC.....	CTTCTCTTGTGTGTTCTT - GGTGTGCTGGTAACC				-5/-1
T0-A11	CCTGCATGGATGTGTTTGATGTCAGCGGAAACC.....	CTTCTCTTGTGTGTTCTGGGTGTGCTGGTAACC				+1/WT
	CCTGCATGGAT --- TTTGATGTCAGCGGAAACC.....	CTTCTCTTGTGTGTTCTT --- TGCTGGTAACC				-3/-5
T0-A12	CCTGCATGGATGTGTTTGATGTCAGCGGAAACC.....	CTTCTCTTGTGTGTTCTGGT - TGCTGGTAACC				-8/-2
	CCTGCATGGATGTGTTTGATGTCAGCGGAAACC.....	CTTCTCTTGTGTGTTCTGGGTGTGCTGGTAACC				WT/+1
T0-A14	CCTGCATGGATGTGTTTGA - TCAGCGGAAACC.....	CTTCTCTTGTGTGTTCTGGT - TGCTGGTAACC				-2/-3
	CCTGCATGGATGTGTTTGATGTCAGCGGAAACC.....	CTTCTCTTGTGTGTTCTGGGTG - TGCTGGTAACC				WT/-1
Target 2 PAM 400bp Target 1 PAM						
WT	CCTGCATGGATGTGTTTGATGTCAGCGGAAACC.....	CTTCTCTTGTGTGTTCTGGGTGTGCTGGTAACC				
T0-B1	CCTGCATGGATGTGTTT --- CAGCGGAAACC					-5/WT/
	CCTGCATGGATGTGTTTGATGTCAGCGGAAACC					
T0-B4	CCTGCATGGATGTGTTTgATGTCAGCGGAAACC					+1/
	CCTGCATGGATGTGTTTG --- TCAGCGGAAACC					-3/
T0-B6	CCTGCATGGATGTGTTTGATG - CAGCGGAAACC					-1/
	CCTGCATGGATGT --- CAGCGGAAACC					-9/
T0-B11	CCTGCATGGATGTGTTTGATGTCAGCGGAAACC					WT/
	CCTGCATGGATGgATGTTTGATGTCAGCGGAAACC					+1/
T0-B12	CCTGCATGGATGTGTTTGATGTCAGCGGAAACC					WT/
	CCTGCATGGATG --- ATGTCAGCGGAAACC					-6/
T0-B14	CCTGCATGGATGTGTTTGATGTCAGCGGAAACC					WT/
	CCTGCATGGATGTGTTTG --- CAGCGGAAACC					-4/
Target 2 PAM 400bp Target 1 PAM						
WT	CCTGCATGGATGTGTTTGATGTCAGCGGAAACC.....	CTTCTCTTGTGTGTTCTGGGTGTGCTGGTAACC				
T0-D1		CTTCTCTTGTGTGTTCTGGT --- TGCTGGTAACC				-3
		CTTCTCTTGTGTGTTCTGGGTGTGCTGGTAACC				/WT
T0-D4		CTTCTCTTGTGTGTTCTT --- TGCTGGTAACC				-5
		CTTCTCTTGTGTGTTCTGGT - TGCTGGTAACC				-1
T0-D6		CTTCTCTTGTGTGTTCTT --- TGCTGGTAACC				-4
		CTTCTCTTGTGTGTTCTGGT - TGCTGGTAACC				-2
T0-D11		CTTCTCTTGTGTGTTCTGGGTGTGCTGGTAACC				+1
		CTTCTCTTGTGTGTTCTGGGTGTGCTGGTAACC				+1
T0-D12		CTTCTCTTGTGTGTTCTGGGTGTGCTGGTAACC				-6
		CTTCTCTTGTGTGTTCTGGGTGTGCTGGTAACC				-6
T0-D14		CTTCTCTTGTGTGTTCTGGGTGTGCTGGTAACC				-2
		CTTCTCTTGTGTGTTCTGGT - TGCTGGTAACC				-2



284 **Figure 5:** CRISPR/Cas9 induced targeted mutagenesis of the *TaRPK1* target gene by LR-2
 285 construct within A, B, and D genomes of wheat T0 plants (**A**). PAM sites were shown in red,
 286 nucleotides in blue denotes target site 1 (T1), and nucleotides in purple represent target site 2
 287 (T2). The lowercase letter denote insertion, dashes represent deletions and dots indicates
 288

289 nucleotides not shown. Spike architecture of wild type and edited transformed LR-1 T0 lines
290 **(B)**. Root architecture of wild type and edited transformed LR-1 T0 lines **(C)**.



292 **Figure 6:** Phenotypic comparison of LR-2 construct for Plant height (cm, **A**), Number of
 293 effective tillers (**B**), Spike length (cm, **C**), Seed weight (g, **D**), Root length (mm, **E**), Root depth
 294 (mm, **F**), Root diameter (mm, **G**), Root volume (mm³, **H**), Root surface area (mm², **I**), and
 295 Root orientation (**J**) of wild type (WT) and edited T0 lines. The data indicates the mean \pm SE
 296 of three biological replicates. Student's *t*-test was used (* = $P < 0.05$, and ** = $P < 0.01$).

297 3.5 Monoallelic and Diallelic mutations in T0 generation

298 ¹ Given the complexity of possible results, from zero to three target sites and using 2
 299 different constructs in complex sub-genomes of hexaploid bread wheat, we have adopted the
 300 terminology of monoallelic (MA) and Diallelic (DA) mutants to define the allelic status of
 301 edited lines. MA mutation means the mutation in one of the homologous copies while DA
 302 mutation means the mutation in both alleles of the target gene (Table 3). Results displayed
 303 higher monoallelic mutation compared to diallelic mutation. 37.5% monoallelic mutation at
 304 target site 1 within the D genome by sgRNA1 was observed by the LR-1 construct (Table 3).
 305 The LR-2 constructs showed a higher monoallelic mutation frequency of 26.67% at target sites
 306 1 and 2 within the A, B, and D genomes (Table 3). The highest diallelic mutation of 25% was
 307 observed at target site 2, by sgRNA2 of LR-1 construct within A genome of wheat. However,
 308 the 20% higher diallelic mutation frequency was detected by sgRNA3 at target site 2 of the
 309 LR-2 construct within the A genome (Table 3).

310 **Table 3.** Summary of CRISPR/Cas9 mutagenesis frequencies in a generation.

Construct	Genome	sgRNA	No. of plants examined	Target sites on T0 plants	Genotype	
					Monoallelic mutation (MA)	Diallelic mutation (DA)
LR-1	A	sgRNA1	16	T 1	05 (31.25%)	02 (12.5%)
		sgRNA2		T 2	03 (18.75%)	04 (25%)
	B	sgRNA2		T 2	04 (25%)	03 (18.75%)
		D		sgRNA1	T 1	06 (37.5%)
	sgRNA2		T 2	04 (25%)	03 (18.75%)	
LR-2	A	sgRNA1	15	T 1	04 (26.67%)	02 (13.33%)
		sgRNA3		T 2	03 (20%)	03 (20%)
	B	sgRNA3		T 2	04 (26.67%)	02 (13.33%)
		D		sgRNA1	T 1	04 (26.67%)

311 3.6 Disruption of *TaRPK1* effects morphological parameters and root system 312 architectural traits

313 To see if *TaRPK1* gene disruption effects the morphological parameters and root system
 314 architecture, we observed and measured these traits in edited lines along with control plants
 315 (Figures 3-6). Alteration in spike architecture in the edited plants was observed (Figure 3B).

316 Measurement of plant height showed that plant height was significantly increased in LR-1
317 edited T0 lines compared with WT plants (Figure 4A). T0-16 and T0-6 lines showed a
318 significant increase in plant height. A maximum number of effective tillers were observed in
319 the T0-16 line followed by T0-6> T0-10> T0-1 LR-1 edited lines (Figure 4B). The rest of the
320 edited lines also showed significant differences in comparison to the WT plants. Spike lengths
321 were reduced significantly in genome-edited LR-1 lines (Figure 4C). A significant reduction
322 in spike length was observed in T0-16 lines followed by T0-6, T0-10, T0-1, and T0-14 lines,
323 respectively. Data regarding 1000 grain weight was significantly increased in all of the T0-
324 edited LR-1 lines with a maximum in T0-16> T0-6> T0-1 lines compared to the control plants
325 (Figure 4D).

326 Similarly, we also observed the plants of the LR-2 construct; an altered spike
327 architecture was noticed in LR-2 edited T0 wheat plants (Figure 5B). The morphological traits³
328 such as the number of effective tillers and plant height were significantly increased, while the
329 spike length was significantly reduced in LR-2 edited wheat T0-1, T0-4, and T0-6 plants. The
330 other edited lines also showed a significant increase in the height of the plant and the effective²
331 number of tillers and decreased spike length compared to WT plants (Figure 6A-C). 1000 grain
332 weight was significantly enhanced in all of T0 edited LR-2 wheat lines (Figure 6D). A
333 significant increase in seed weight was detected in all LR-2 T0 edited lines, with the highest in
334 T0-1, T0-4, and T0-6 lines.

335 The root architectural traits showed significant effects in LR-1 genome-edited T0 lines
336 (Figure 3C). The root length, root depth, volume, and surface area were significantly increased
337 (Figures 4E-F and H-I), however, the root diameter and root angle were significantly reduced
338 in genome-edited LR-1 (Figure 4G and 4J) T0 lines compared to the WT plants. T0-1, T0-6,
339 T0-10, and T0-16 lines displayed very significant differences in comparison to the control
340 plants. However, in comparison to the wild-type plants, the other T0 lines also exhibited
341 significant differences. An altered architecture of roots was observed in LR-1 edited T0 wheat
342 plants (Figure 3C). Similarly, in the other construct (LR-2), root architectural traits also
343 displayed significant variations in genome-edited T0 lines (Figure 5C). The root length, depth,
344 surface area, and volume were significantly enhanced (Figures 6E-F and H-I). However, the
345 root diameter and root angle were reduced significantly in genome-edited LR-2 T0 lines
346 (Figure 6G and 6J). T0-1, T0-4, and T0-6 lines displayed very significant differences as
347 compared to the WT plants. However, in comparison to the WT plants, the other T0 lines also
348 exhibited significant differences.

349 Notably, the alterations detected in transgenic edited lines compared to WT plants have
350 occurred due to editing of *TaRPK1* genes in wheat based on specific targeted designed sgRNAs
351 that might have altered the open reading frame and hence the amino acid sequence
352 (Supplementary Figure S4). The observed reduction in spike length, root diameter, and root
353 angle, and enhanced root length, depth, surface area, and volume, results in a significant
354 upsurge in the number of effective tillers and grain weight, compared to WT plants. This
355 increase in grain weight and the number of effective tillers proposed that edited lines
356 recompense the grain yield reduction caused due to decreased spike length. This study reveals
357 that *TaRPK1* editing results in the improvement of root architecture traits and hence yield
358 enhancement.

359 **4. Discussion**

360 Common wheat is an essential crop and has a complex genome comprising of A, B, and
361 D sub-genomes (Zhang et al., 2018). The complexity of the wheat genome in comparison to
362 other plants such as Arabidopsis, rice, and maize makes it a challenging and vital crop for
363 researchers and scientists to study and optimize genome editing systems (Zhang et al., 2019).
364 The CRISPR/Cas9 system has advanced promptly recently (Ma and Liu 2016). In this study,
365 we have targeted *TaRPK1* genes in wheat using CRISPR/Cas9 (Figure 1), which involves all
366 of the steps from the design of sgRNA to agronomic traits analysis across T0 generation.

367 CRISPR/Cas9 has been used to generate double-strand breaks (DSBs) within the host
368 genome, which is similar to other site-specific nucleases such as meganucleases, ZFNs, and
369 TALENs. The principal repair mechanism is the Non-Homologous End Joining (NHEJ)
370 mechanism. The NHEJ-based small insertion/deletions (indels) mutagenesis is the most
371 important genome editing application (Sander and Joung 2014). The frequency of NHEJ-
372 mediated mutagenesis is influenced by a variety of factors. The major factors affecting the rate
373 of this efficiency are the spatiotemporal expression of sgRNAs and Cas9 by promoters,
374 selection of sgRNA, delivery methods of sgRNA /Cas9/ which leads to different numbers of
375 transgenic copies, and, the sequence of a gene and its chromosomal position that affects the
376 target gene accessibility of sgRNA/Cas9 complex to create DSBs (Wu et al., 2014, Horlbeck
377 et al., 2016).

378 *Agrobacterium tumefaciens* and biolistic bombardment are the effective and major
379 methods for wheat transformation. As the efficiency of editing is also governed by complex
380 delivery, most of the CRISPR/Cas editing was performed by the biolistic transformation in

381 wheat (Wang et al., 2014, Liang et al., 2017, Hamada et al., 2018, Wang et al., 2018). The
382 major challenge is that the gene gun transformation involves numerous embryos, and for the
383 editing events that take place during CRISPR/Cas9 transient expression, the CRISPR/Cas9 and
384 selection marker cassette is not incorporated within the genome. This creates several transgene
385 copies with a high gene silencing frequency and low rate of editing. In comparison,
386 *Agrobacterium*-mediated transformation is less costly as it does not involve expensive
387 apparatus and supplies. This method is the most prevalent because it involves the insertion of
388 single or few copies of transgenes, hence mutations are induced with high efficiency and show
389 stable heritability in wheat (Zhang et al., 2019). This study involves the application of
390 CRISPR/Cas9 by *Agrobacterium tumefaciens*-mediated method for editing the genome at its
391 specific target sites in wheat.

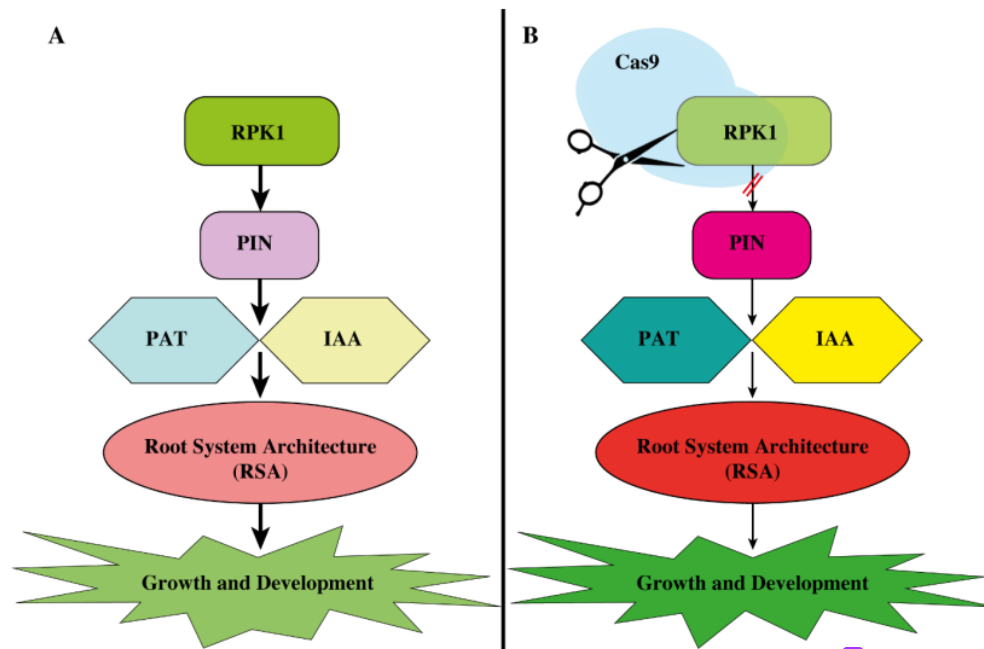
392 We adopted the two-sgRNAs-for-one-gene approach to enhance presumably double the
393 rate of success or improve the probability of activation of at least one of the gRNA for
394 mutagenesis, as reported in previous studies that not every synthesized sgRNA is highly active
395 or active to create DSBs (Schmitz et al., 2020). This approach would enhance the attainment
396 of targeted mutagenesis and larger deletion mutations (Char et al., 2017).

397 The target site selection is a crucial step. The gRNAs GC content is essential for the
398 CRISPR/Cas9 efficiency (Wang et al., 2014, Zhang et al., 2018). In our study, the percentage
399 of GC content in sgRNA1 and sgRNA3 was 41.67%, and in gRNA2 was 45.83% (Table 2).
400 The gRNA2 having higher GC% content exhibited a higher efficiency (Zhang et al., 2018).
401 The base composition and position of the gRNA may also affect CRISPR/Cas9 efficiency.
402 Furthermore, chromatin availability is accompanied by the efficiency of CRISPR/Cas9 as
403 reported in the zebrafish and human cells (Daer et al., 2017, Kallimasioti-Pazi et al., 2018,
404 Uusi-Mäkelä et al., 2018). The efficiency of editing may be associated with the target genes'
405 chromatin state (Zhang et al., 2019).

406 In the present study, we synthesized two constructs namely LR-1 and LR-2, with two
407 gRNAs each, and successfully created mutagenesis in target sites of *TaRPK1* genes, via
408 *Agrobacterium*-mediated CRISPR/Cas9 in T0 plants. Our results indicated that the primary
409 mutation type was deletion. Similar observations were also reported in other wheat studies
410 (Wang et al., 2014, Liang et al., 2017, Sanchez-Leon et al., 2018, Wang et al., 2018, Zhang et
411 al., 2018, Zhang et al., 2019, Zhang et al., 2019, Ibrahim et al., 2022). However, these
412 observations contradict with rice, where insertion is the dominant mutation type (Zhang et al.,

413 2014). We reported that the CRISPR/Cas9 system can achieve efficiently specific targeted
414 editing with a mutation frequency of 43.75% and 40% for LR-1 and LR-2 constructs,
415 respectively (Table 2). The stated efficiencies of mutations within different species or even
416 different CRISPR platforms within wheat vary significantly. For instance, a relatively lower
417 editing frequency of 5.6%, to 20.8%–54.2% mutation efficiency was reported in T0 wheat
418 plants (Zhang et al., 2019). 54.17% mutagenesis efficiency which was much higher than earlier
419 reported mutation frequency was also stated in larger and more complex genome cereal crops,
420 and wheat (Zhang et al., 2018). In contrast, a significant rate of editing up to 100% have been
421 reported by several laboratories working on rice (Zhang et al., 2014, Zou et al., 2014, Viana et
422 al., 2019). In dicotyledonous crops, such as soybean and tomato, CRISPR systems generated
423 higher than 50% mutation in T0 plants (Brooks et al., 2014, Li et al., 2015). In maize, 2%–
424 100% editing efficiency was reported in the T0 plants (Liang et al., 2014, Xing et al., 2014,
425 Svitashv et al., 2015, Feng et al., 2016, Zhu et al., 2016, Char et al., 2017).

426 *RPKI* is one of the many genes that modulate the abiotic stresses and root system
427 architecture (RSA), hence affecting yield. Our results are in corroborate the previous study
428 performed on rice, where the knockdown of rice improved the root system architecture, and
429 increased tillering numbers and plant height (Zou et al., 2014). Similar results with alterations
430 in root system architecture, spike architecture, increased numbers of tillers, plant height, and
431 grain weight were observed through CRISPR/Cas9 knockdown of the *TaRPKI* gene in T0 lines
432 of wheat. The LR-1 and LR-2 T0 lines exhibited a significant alteration in morphological and
433 architectural traits compared to WT plants due to modification in amino acid sequence and
434 hence structure and function of TaRPK1 protein due to insertions and deletions caused by
435 CRISPR/Cas9 mediated genome editing. Increased root architectural traits such as root length,
436 depth, volume, and surface area, were exhibited, while decreased root angle and diameter were
437 observed compared to the WT plants in CRISPR/Cas9 knockdown lines. As reported, these
438 variations in the root architecture and their interplay with the shoot system attribute features to
439 face water scarcity during drought stress and maintain yield (Siddiqui et al., 2021). The
440 mechanism of how *RPKI* affects root system architecture might be via negative modulation of
441 polar auxin transport (Figure 7).



442

443 **Figure 7.** Involvement of *RPK1* in root system architecture regulation. (A) Schematic
 444 illustration of normal *RPK1* pathway, in which *RPK1* is normally expressed and inhibits the
 445 expression of other genes such as *PIN*, *IAA*, and *PAT*. This less expression leads to poor root
 446 development. (B) Editing of *RPK1* by using the Cas9 system leads to less expression of *RPK1*
 447 and higher expression of *PIN*, *PAT*, and *IAA*. This causes the proper or better root development
 448 under drought stress.

449 **5. Conclusion**

450 In summary, the CRISPR/Cas9 system was highly efficient in generating *TaRPK1* gene
 451 editing in wheat. Mutant lines harboring the desired modification in *TaRPK1* were obtained.
 452 The edited lines displayed altered root architectural and agronomic traits. This study has
 453 potential application in raising efforts to produce valuable traits in bread wheat. Our work
 454 presents a positive illustration of the CRISPR application, the precision and rapidity with which
 455 variations can be attained by this approach will assist in wheat improvement at a rate sufficient
 456 to assure food security globally.

457 **Funding:**

458

459 **Acknowledgments:**

460 **Author contributions:**

461 **Availability of data and materials:** ³ All the data is presented in the main text and
462 [supplementary files](#). Further materials can be demanded from the corresponding author.

463 **Supplementary Material:**

464 **Supplementary Table S1:** The RPK1 sequences in the ¹ A, B, and D sub-genomes of wheat.

465 **Supplementary Table S2:** Alignment of A, B, and D CDS genomes.

466 **Supplementary Table S3:** Primer sequences used for sequencing of A, B, and D genomes.

467 **Supplementary Figure S1:** A flowchart of targeted mutagenesis in bread wheat.

468 **Supplementary Figure S2:** Construction of gRNA expression cassettes.

469 **Supplementary Figure S3:** Genomic DNA of control (1) and transgenic plants (2-4). The
470 marker was denoted with “M”.

471 **Supplementary Figure S4:** Multiple sequence alignment of TaRPK1 proteins depicting
472 structural predictions.

473 **Ethics declarations**

474 **Ethical approval and consent to participate:** Not applicable.

475 **Consent to publish:** Not applicable.

476 **Competing interests**

477 The authors declare that they have no competing interests.

478 **References**

479 Abdul, R., Ishfaq, A.H., Imran, M., Azhar, H., 2011. Development of in planta transformation protocol
480 for wheat. *African Journal of Biotechnology*.

481 Abe, F., Haque, E., Hisano, H., Tanaka, T., Kamiya, Y., Mikami, M., Kawaura, K., Endo, M., Onishi, K.,
482 Hayashi, T., 2019. Genome-edited triple-recessive mutation alters seed dormancy in wheat.
483 *Cell reports*.
484

485 Alahmad, S., El Hassouni, K., Bassi, F.M., Dinglasan, E., Youssef, C., Quarry, G., Aksoy, A., Mazzucotelli,
486 E., Juhász, A., Able, J.A., 2019. A major root architecture qtl responding to water limitation in
487 durum wheat. *Frontiers in Plant Science*.
488

489 Bishopp, A., Lynch, J.P., 2015. The hidden half of crop yields. *Nature Plants*.

491 Brandt, K.M., Gunn, H., Moretti, N., Zemetra, R.S., 2020. A streamlined protocol for wheat (*triticum*
492 *aestivum*) protoplast isolation and transformation with crispr-cas ribonucleoprotein
493 complexes. *Frontiers in Plant Science*.
494

495 Brooks, C., Nekrasov, V., Lippman, Z.B., Van Eck, J., 2014. Efficient gene editing in tomato in the first
496 generation using the clustered regularly interspaced short palindromic repeats/crispr-
497 associated9 system. *Plant physiology*.
498

499
500 Char, S.N., Li, R., Yang, B., 2019. Crispr/cas9 for mutagenesis in rice. *Transgenic plants*, Springer: 279-
501 293.

502
503 Char, S.N., Neelakandan, A.K., Nahampun, H., Frame, B., Main, M., Spalding, M.H., Becraft, P.W.,
504 Meyers, B.C., Walbot, V., Wang, K., 2017. An agrobacterium-delivered crispr/cas9 system for
505 high-frequency targeted mutagenesis in maize. *Plant biotechnology journal*.

506
507 Chen, W., Jin, M., Ferré, T.P., Liu, Y., Huang, J., Xian, Y., 2020. Soil conditions affect cotton root
508 distribution and cotton yield under mulched drip irrigation. *Field Crops Research*.

509
510 Daer, R.M., Cutts, J.P., Brafman, D.A., Haynes, K.A., 2017. The impact of chromatin dynamics on cas9-
511 mediated genome editing in human cells. *ACS synthetic biology*.

512
513 Dai, C., Lee, Y., Lee, I.C., Nam, H.G., Kwak, J.M., 2018. Calmodulin 1 regulates senescence and aba
514 response in arabidopsis. *Frontiers in Plant Science*.

515
516 Danakumara, T., Kumari, J., Singh, A.K., Sinha, S.K., Pradhan, A.K., Sharma, S., Jha, S.K., Bansal, R.,
517 Kumar, S., Jha, G.K., 2021. Genetic dissection of seedling root system architectural traits in a
518 diverse panel of hexaploid wheat through multi-locus genome-wide association mapping for
519 improving drought tolerance. *International journal of molecular sciences*.

520
521 Djanaguiraman, M., Prasad, P., Kumari, J., Rengel, Z., 2019. Root length and root lipid composition
522 contribute to drought tolerance of winter and spring wheat. *Plant and Soil*.

523
524 Djanaguiraman, M., Prasad, P., Kumari, J., Sehgal, S., Friebe, B., Djalovic, I., Chen, Y., Siddique, K.H.,
525 Gill, B., 2019. Alien chromosome segment from *aegilops speltoides* and *dasyphyrum villosum*
526 increases drought tolerance in wheat via profuse and deep root system. *BMC plant biology*.

527
528 El Hassouni, K., Alahmad, S., Belkadi, B., Filali-Maltouf, A., Hickey, L., Bassi, F., 2018. Root system
529 architecture and its association with yield under different water regimes in durum wheat. *Crop*
530 *Science*.

531
532 Feng, C., Yuan, J., Wang, R., Liu, Y., Birchler, J.A., Han, F., 2016. Efficient targeted genome modification
533 in maize using crispr/cas9 system. *Journal of Genetics and Genomics*.

534
535 Feng, Z., Zhang, B., Ding, W., Liu, X., Yang, D.-L., Wei, P., Cao, F., Zhu, S., Zhang, F., Mao, Y., 2013.
536 Efficient genome editing in plants using a crispr/cas system. *Cell research*.

537
538 Fradgley, N., Evans, G., Biernaskie, J., Cockram, J., Marr, E., Oliver, A., Ober, E., Jones, H., 2020. Effects
539 of breeding history and crop management on the root architecture of wheat. *Plant and Soil*.

540

541 Gabay, G., Wang, H., Zhang, J., Moriconi, J.I., Burguener, G.F., Gualano, L.D., Howell, T., Lukaszewski,
542 A., Staskawicz, B., Cho, M.-J., 2023. Dosage differences in 12-oxophytodienoate reductase
543 genes modulate wheat root growth. *Nature communications*.

544
545 Hamada, A., Nitta, M., Nasuda, S., Kato, K., Fujita, M., Matsunaka, H., Okumoto, Y., 2011. Novel qtls
546 for growth angle of seminal roots in wheat. *Plant and Soil*.

547
548 Hamada, H., Liu, Y., Nagira, Y., Miki, R., Taoka, N., Imai, R., 2018. Biolistic-delivery-based transient
549 crispr/cas9 expression enables in planta genome editing in wheat. *Scientific reports*.

550
551 Hong, S.W., Jon, J.H., Kwak, J.M., Nam, H.G., 1997. Identification of a receptor-like protein kinase gene
552 rapidly induced by abscisic acid, dehydration, high salt, and cold treatments in *arabidopsis*
553 *thaliana*. *Plant physiology*.

554
555 Horlbeck, M.A., Witkowsky, L.B., Guglielmi, B., Replogle, J.M., Gilbert, L.A., Villalta, J.E., Torigoe, S.E.,
556 Tjian, R., Weissman, J.S., 2016. Nucleosomes impede cas9 access to DNA in vivo and in vitro.
557 *elife*.

558
559 Ibrahim, S., Saleem, B., Rehman, N., Zafar, S.A., Naeem, M.K., Khan, M.R., 2022. Crispr/cas9 mediated
560 disruption of inositol pentakisphosphate 2-kinase 1 (*taipk1*) reduces phytic acid and improves
561 iron and zinc accumulation in wheat grains. *Journal of advanced research*.

562
563 Javaux, M., Couvreur, V., Vanderborght, J., Vereecken, H., 2013. Root water uptake: From three-
564 dimensional biophysical processes to macroscopic modeling approaches. *Vadose Zone*
565 *Journal*.

566
567 Kallimasioti-Pazi, E.M., Thelakkad Chathoth, K., Taylor, G.C., Meynert, A., Ballinger, T., Kelder, M.J.,
568 Lalevée, S., Sanli, I., Feil, R., Wood, A.J., 2018. Heterochromatin delays crispr-cas9 mutagenesis
569 but does not influence the outcome of mutagenic DNA repair. *PLoS Biology*.

570
571 Kim, D., Alptekin, B., Budak, H., 2018. Crispr/cas9 genome editing in wheat. *Functional & integrative*
572 *genomics*.

573
574 Kim, K., Shin, J., Kang, T.-A., Kim, B., Kim, W.-C., 2023. Crispr/cas9-mediated *atgata25* mutant
575 represents a novel model for regulating hypocotyl elongation in *arabidopsis thaliana*.
576 *Molecular Biology Reports*.

577
578 Lee, I.C., Hong, S.W., Whang, S.S., Lim, P.O., Nam, H.G., Koo, J.C., 2011. Age-dependent action of an
579 aba-inducible receptor kinase, *rpk1*, as a positive regulator of senescence in *arabidopsis*
580 leaves. *Plant and Cell physiology*.

581
582 Li, J., Li, Y., Ma, L., 2019. Crispr/cas9-based genome editing and its applications for functional genomic
583 analyses in plants. *Small Methods*.

584

585 Li, Z., Liu, Z.-B., Xing, A., Moon, B.P., Koellhoffer, J.P., Huang, L., Ward, R.T., Clifton, E., Falco, S.C., Cigan,
586 A.M., 2015. Cas9-guide rna directed genome editing in soybean. *Plant physiology*.

587
588 Liang, Z., Chen, K., Li, T., Zhang, Y., Wang, Y., Zhao, Q., Liu, J., Zhang, H., Liu, C., Ran, Y., 2017. Efficient
589 DNA-free genome editing of bread wheat using crispr/cas9 ribonucleoprotein complexes.
590 *Nature communications*.

591
592 Liang, Z., Zhang, K., Chen, K., Gao, C., 2014. Targeted mutagenesis in zea mays using talens and the
593 crispr/cas system. *Journal of Genetics and Genomics*.

594
595 Lv, J., Yu, K., Wei, J., Gui, H., Liu, C., Liang, D., Wang, Y., Zhou, H., Carlin, R., Rich, R., 2020. Generation
596 of paternal haploids in wheat by genome editing of the centromeric histone cenH3. *Nature*
597 *biotechnology*.

598
599 Ma, X., Liu, Y.G., 2016. Crispr/cas9-based multiplex genome editing in monocot and dicot plants.
600 *Current protocols in molecular biology*.

601
602 Maccaferri, M., El-Feki, W., Nazemi, G., Salvi, S., Canè, M.A., Colalongo, M.C., Stefanelli, S., Tuberosa,
603 R., 2016. Prioritizing quantitative trait loci for root system architecture in tetraploid wheat.
604 *Journal of experimental botany*.

605
606 Malzahn, A.A., Tang, X., Lee, K., Ren, Q., Sretenovic, S., Zhang, Y., Chen, H., Kang, M., Bao, Y., Zheng,
607 X., Deng, K., Zhang, T., Salcedo, V., Wang, K., Zhang, Y., Qi, Y., 2019. Application of crispr-
608 cas12a temperature sensitivity for improved genome editing in rice, maize, and arabidopsis.
609 *BMC Biol.* <https://doi.org/10.1186/s12915-019-0629-5>

610
611 Mohr, T., Horstman, J., Gu, Y.Q., Elarabi, N.I., Abdallah, N.A., Thilmony, R., 2022. Crispr-cas9 gene
612 editing of the sal1 gene family in wheat. *Plants*.

613
614 Murashige, T., Skoog, F., 1962. A revised medium for rapid growth and bio assays with tobacco tissue
615 cultures. *Physiologia plantarum*.

616
617 Nehe, A.S., Foulkes, M.J., Ozturk, I., Rasheed, A., York, L., Kefauver, S.C., Ozdemir, F., Morgounov, A.,
618 2021. Root and canopy traits and adaptability genes explain drought tolerance responses in
619 winter wheat. *PLoS One*. <https://doi.org/10.1371/journal.pone.0242472>

620
621 Nekrasov, V., Staskawicz, B., Weigel, D., Jones, J.D., Kamoun, S., 2013. Targeted mutagenesis in the
622 model plant *Nicotiana benthamiana* using cas9 rna-guided endonuclease. *Nature*
623 *biotechnology*.

624
625 Nodine, M.D., Tax, F.E., 2008. Two receptor-like kinases required together for the establishment of
626 arabidopsis cotyledon primordia. *Dev Biol.* <https://doi.org/10.1016/j.ydbio.2007.11.021>

627

628 Nodine, M.D., Yadegari, R., Tax, F.E., 2007. Rpk1 and toad2 are two receptor-like kinases redundantly
629 required for arabidopsis embryonic pattern formation. Dev Cell.
630 <https://doi.org/10.1016/j.devcel.2007.04.003>

631

632 Ober, E.S., Alahmad, S., Cockram, J., Forestan, C., Hickey, L.T., Kant, J., Maccaferri, M., Marr, E., Milner,
633 M., Pinto, F., 2021. Wheat root systems as a breeding target for climate resilience. Theoretical
634 and Applied Genetics.

635

636 Rahim, A.A., Uzair, M., Rehman, N., Rehman, O.U., Zahra, N., Khan, M.R., 2022. Genome-wide
637 identification and characterization of *receptor-like protein kinase 1 (rpk1)* gene family in
638 *triticum aestivum* under drought stress. Frontiers in genetics.

639

640 Rufo, R., Salvi, S., Royo, C., Soriano, J.M., 2020. Exploring the genetic architecture of root-related traits
641 in mediterranean bread wheat landraces by genome-wide association analysis. Agronomy.

642

643 Sanchez-Leon, S., Gil-Humanes, J., Ozuna, C.V., Gimenez, M.J., Sousa, C., Voytas, D.F., Barro, F., 2018.
644 Low-gluten, nontransgenic wheat engineered with crispr/cas9. Plant Biotechnol J.
645 <https://doi.org/10.1111/pbi.12837>

646

647 Sander, J.D., Joung, J.K., 2014. Crispr-cas systems for editing, regulating and targeting genomes.
648 Nature biotechnology.

649

650 Schilling, S., Kennedy, A., Pan, S., Jermiin, L.S., Melzer, R., 2020. Genome-wide analysis of mick-type
651 mads-box genes in wheat: Pervasive duplications, functional conservation and putative
652 neofunctionalization. New Phytologist.

653

654 Schmitz, D.J., Ali, Z., Wang, C., Aljedaani, F., Hooykaas, P.J., Mahfouz, M., de Pater, S., 2020. Crispr/cas9
655 mutagenesis by translocation of cas9 protein into plant cells via the agrobacterium type iv
656 secretion system. Frontiers in genome editing.

657

658 Seethepalli, A., Dhakal, K., Griffiths, M., Guo, H., Freschet, G.T., York, L.M., 2021. Rhizovision explorer:
659 Open-source software for root image analysis and measurement standardization. AoB plants.

660

661 Shi, C.-C., Feng, C.-C., Yang, M.-M., Li, J.-L., Li, X.-X., Zhao, B.-C., Huang, Z.-J., Ge, R.-C., 2014.
662 Overexpression of the receptor-like protein kinase genes *atrpk1* and *osrpk1* reduces the salt
663 tolerance of *arabidopsis thaliana*. Plant Science.

664

665 Siddiqui, M.N., Léon, J., Naz, A.A., Ballvora, A., 2021. Genetics and genomics of root system variation
666 in adaptation to drought stress in cereal crops. Journal of experimental botany.

667

668 Supartana, P., Shimizu, T., Shioiri, H., Nogawa, M., Nozue, M., Kojima, M., 2005. Development of
669 simple and efficient in planta transformation method for rice (*oryza sativa* L.) using
670 *agrobacterium tumefaciens*. Journal of bioscience and bioengineering.

671

672 Svitashv, S., Young, J.K., Schwartz, C., Gao, H., Falco, S.C., Cigan, A.M., 2015. Targeted mutagenesis,
673 precise gene editing, and site-specific gene insertion in maize using cas9 and guide rna. Plant
674 physiology.

675

676 Uusi-Mäkelä, M.I., Barker, H.R., Bäuerlein, C.A., Häkkinen, T., Nykter, M., Rämetsä, M., 2018. Chromatin
677 accessibility is associated with crispr-cas9 efficiency in the zebrafish (*danio rerio*). PloS One.

678

679 Uzair, M., Long, H., Zafar, S.A., Patil, S.B., Chun, Y., Li, L., Fang, J., Zhao, J., Peng, L., Yuan, S., 2021.
680 *Narrow leaf21*, encoding ribosomal protein rps3a, controls leaf development in rice. Plant
681 physiology.

682

683 Viana, V.E., Pegoraro, C., Busanello, C., Costa de Oliveira, A., 2019. Mutagenesis in rice: The basis for
684 breeding a new super plant. Frontiers in Plant Science.

685

686 Wang, W., Pan, Q., He, F., Akhunova, A., Chao, S., Trick, H., Akhunov, E., 2018. Transgenerational
687 crispr-cas9 activity facilitates multiplex gene editing in allopolyploid wheat. The CRISPR
688 journal.

689

690 Wang, W., Simmonds, J., Pan, Q., Davidson, D., He, F., Battal, A., Akhunova, A., Trick, H.N., Uauy, C.,
691 Akhunov, E., 2018. Gene editing and mutagenesis reveal inter-cultivar differences and
692 additivity in the contribution of tagw2 homoeologues to grain size and weight in wheat.
693 Theoretical and Applied Genetics.

694

695 Wang, Y., Cheng, X., Shan, Q., Zhang, Y., Liu, J., Gao, C., Qiu, J.-L., 2014. Simultaneous editing of three
696 homoeoalleles in hexaploid bread wheat confers heritable resistance to powdery mildew.
697 Nature biotechnology.

698

699 Wu, X., Scott, D.A., Kriz, A.J., Chiu, A.C., Hsu, P.D., Dadon, D.B., Cheng, A.W., Trevino, A.E., Konermann,
700 S., Chen, S., 2014. Genome-wide binding of the crispr endonuclease cas9 in mammalian cells.
701 Nature biotechnology.

702

703 Xing, H.-L., Dong, L., Wang, Z.-P., Zhang, H.-Y., Han, C.-Y., Liu, B., Wang, X.-C., Chen, Q.-J., 2014. A
704 crispr/cas9 toolkit for multiplex genome editing in plants. BMC plant biology.

705

706 Zafar, K., Khan, M.Z., Amin, I., Mukhtar, Z., Yasmin, S., Arif, M., Ejaz, K., Mansoor, S., 2020. Precise
707 crispr-cas9 mediated genome editing in super basmati rice for resistance against bacterial
708 blight by targeting the major susceptibility gene. Frontiers in Plant Science.

709

710 Zhang, H., Zhang, J., Wei, P., Zhang, B., Gou, F., Feng, Z., Mao, Y., Yang, L., Zhang, H., Xu, N., 2014. The
711 crispr/cas9 system produces specific and homozygous targeted gene editing in rice in one
712 generation. Plant biotechnology journal.

713

714 Zhang, S., Zhang, R., Gao, J., Gu, T., Song, G., Li, W., Li, D., Li, Y., Li, G., 2019. Highly efficient and
715 heritable targeted mutagenesis in wheat via the agrobacterium tumefaciens-mediated
716 crispr/cas9 system. International journal of molecular sciences.

717

718 Zhang, S., Zhang, R., Song, G., Gao, J., Li, W., Han, X., Chen, M., Li, Y., Li, G., 2018. Targeted mutagenesis
719 using the agrobacterium tumefaciens-mediated crispr-cas9 system in common wheat. BMC
720 plant biology.

721

722 Zhang, Y., Li, D., Zhang, D., Zhao, X., Cao, X., Dong, L., Liu, J., Chen, K., Zhang, H., Gao, C., 2018. Analysis
723 of the functions of ta gw 2 homoeologs in wheat grain weight and protein content traits. The
724 Plant Journal.

725

726 Zhang, Z., Hua, L., Gupta, A., Tricoli, D., Edwards, K.J., Yang, B., Li, W., 2019. Development of an
727 agrobacterium-delivered crispr/cas9 system for wheat genome editing. Plant biotechnology
728 journal.

729

730 Zhu, J., Song, N., Sun, S., Yang, W., Zhao, H., Song, W., Lai, J., 2016. Efficiency and inheritance of
731 targeted mutagenesis in maize using crispr-cas9. Journal of Genetics and Genomics.

732

733 Zou, Y., Liu, X., Wang, Q., Chen, Y., Liu, C., Qiu, Y., Zhang, W., 2014. *Osrpk1*, a novel leucine-rich repeat
734 receptor-like kinase, negatively regulates polar auxin transport and root development in rice.
735 Biochimica et Biophysica Acta (BBA)-General Subjects.

736

737

ORIGINALITY REPORT

8%

SIMILARITY INDEX

7%

INTERNET SOURCES

7%

PUBLICATIONS

0%

STUDENT PAPERS

PRIMARY SOURCES

1	onlinelibrary.wiley.com Internet Source	2%
2	www.ncbi.nlm.nih.gov Internet Source	1%
3	link.springer.com Internet Source	1%
4	Mark A. Smedley, Sadiye Hayta, Martha Clarke, Wendy A. Harwood. "CRISPR-Cas9 Based Genome Editing in Wheat", Current Protocols, 2021 Publication	1%
5	Saira Ibrahim, Bilal Saleem, Nazia Rehman, Syed Adeel Zafar, Muhammad Kashif Naeem, Muhammad Ramzan Khan. "CRISPR/Cas9 mediated disruption of Inositol Pentakisphosphate 2-Kinase 1 (TaIPK1) reduces phytic acid and improves iron and zinc accumulation in wheat grains", Journal of Advanced Research, 2021 Publication	1%

6

Susanne Schilling, Alice Kennedy, Sirui Pan, Lars S. Jermiin, Rainer Melzer. " Genome-wide analysis of -type -box genes in wheat: pervasive duplications, functional conservation and putative neofunctionalization ", New Phytologist, 2019
Publication

1 %

Exclude quotes Off

Exclude matches < 1%

Exclude bibliography On